Journal of Structural Geology 31 (2009) 1074–1083

Contents lists available at ScienceDirect

Journal of Structural Geology

journal homepage: www.elsevier.com/locate/jsg

Constraining neotectonic orogenesis using an isostatically compensated model of transpression

Scott Giorgis*, John Tong [1], Robert Sirianni [2]

Department of Geological Sciences, SUNY-Geneseo, 1 College Circle, Geneseo, NY 14414, USA

ARTICLE INFO

Article history:
Received 29 May 2008
Received in revised form
12 February 2009
Accepted 13 February 2009
Available online 4 March 2009

Keywords:
Transpression
Strain
Isostasy
Erosion
Alpine fault
New Zealand
Central Range fault
Trinidad

ABSTRACT

Current models of transpression allow upward flow of material to compensate for shortening in the horizontal plane. We present an isostatically compensated model of transpression, where material is allowed to flow both upwards to create topographic relief and downwards to form a crustal root. Our model also incorporates the effects of erosion to more accurately examine the developing topography in orogenic systems. The modeling results suggest that topographic relief and crustal root thickness developed in transpressional orogens are most dependent on the magnitude of shortening, the initial thickness of the crust, and the density contrast between the crust and mantle. In contrast, the rate of convergence and final width of the deformed zone are relatively unimportant parameters in this model. Application to the Alpine fault system in New Zealand, a well-constrained active transpressional plate boundary, shows good agreement between topography-based model estimates of shortening and those derived from plate reconstructions. Application of our model to the Central Range fault zone in Trinidad suggests 2 ± 1 km of neotectonic shortening. The strain analysis approach presented here may be useful for isolating the effects of modern deformation in a region that has reactivated an ancient contractional belt.

1. Introduction

There is a well established interaction and feedback between landscape evolution and tectonic convergence (e.g. Willett, 1999; Willett and Brandon, 2002). In active mountain belts, an intuitive relationship exists between the amount of shortening and the topographic relief of an orogen. For example, the convergence along the Alpine fault (e.g. Walcott, 1998) that created the Southern Alps is much greater than that responsible for the rolling hills of the central Coast Ranges in the San Andreas fault system (e.g. Argus and Gordon, 2001). This relationship occurs throughout the San Andreas system where changes in the fault orientation along strike change the relative rates of convergent vs. strike-slip motion. Those areas that experience greater rates of convergent motion tend to be characterized by greater topographic relief; conversely, those areas dominated by strike-slip motion tend to have lower relief (e.g. Argus and Gordon, 2001; Spotila et al., 2007).

Obliquely convergent orogens such as the Alpine fault or the San Andreas fault zones are typically modeled as transpressional systems (e.g. Little et al., 2002; Teyssier and Tikoff, 1998). Transpression involves simultaneous strike-slip and convergent motion in a horizontal plane coupled with vertical elongation to compensate for the horizontal shortening (Fig. 1). In most models of transpression, vertical elongation is accommodated by movement of material upwards towards the Earth's surface (e.g. Sanderson and Marchini, 1984; Robin and Cruden, 1994; Thompson et al., 1997; Dewey et al., 1998). Application of transpression to the plate boundary scale leads to the development of topography, but this topography must be balanced by isostatic compensation (e.g. Stüwe and Barr, 1998). Additionally, the topographic relief created by convergence is continuously reduced by erosion, resulting in a feedback between isostatic and erosive affects (e.g. Stüwe and Barr, 1998). Therefore development of a quantitatively meaningful relationship between tectonic convergence and topographic relief requires a model of transpression that incorporates both isostatic compensation and erosion.

In this contribution, we present a model of transpression that links topographic relief and crustal root formation to tectonic shortening by incorporating both isostasy and erosion. We focus

* Corresponding author. Tel.: +1 585 245 5293.
E-mail addresses: giorgis@geneseo.edu (S. Giorgis), jjtong@gmail.com (J. Tong), rsirianni@ufl.edu (R. Sirianni).
[1] Present address: The Department of Geology & Geophysics, Texas A&M University, College Station, TX 77843-3115, USA.
[2] Present address: University of Florida, Department of Geological Sciences, 241 Williamson Hall, P.O. Box 112120, Gainesville, FL 32611, USA.

0191-8141/$ – see front matter © 2009 Elsevier Ltd. All rights reserved.
doi:10.1016/j.jsg.2009.02.003

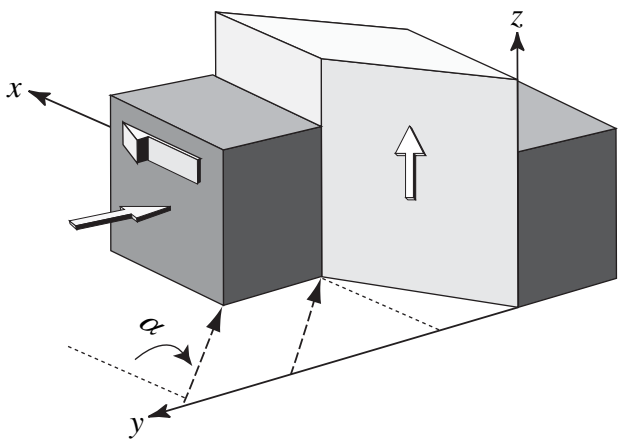

Fig. 1. Transpression results in wrenching parallel to plate margin (*x*-axis), shortening across shear zone (*y*-axis), and vertical extrusion (*z*-axis).

on transpressional settings because tectonic contraction is most often accommodated on obliquely convergence boundaries (e.g. Dewey et al., 1998). Moreover, the pure shear nature of convergence in transpression allows for the development of straightforward relationships between shortening, topography, crustal root formation, and erosion. Previous studies have developed more complex simulations of these relationships that include additional variables to model a variety of processes. For example, Beaumont et al. (1992) investigated the orographic effects of rain shadows. Koons (1994) examined the interaction of shortening, mountain building, and erosion in the context of a three-dimensional critical wedge. Willett (1999) explored the effects of climate, rock erodibility, and precipitation rate using a finite element model. Willett and Brandon (2002) examined steady vs. non-steady-state evolution of mountain belts. The model presented here complements these more complex investigations in two ways. First, these more complex models do not investigate the effects of isostatic compensation and erosion in oblique convergence using the simple kinematic framework of transpression. Second, our model provides a simple method for using widely available data sets (elevation and/or gravity) to generate first-order estimates of shortening in neotectonic, transpressional settings.

2. Numerical model

Fig. 2 outlines our approach to integrating isostasy and erosion into transpression. We begin with an initially undeformed block of continental crust. This crustal block starts at an isostatic equilibrium position governed by its initial thickness. The top of this block is flat and at an elevation equal to base level (i.e. sea level for many orogens). Shortening thickens the crustal block, which changes the equilibrium position. The increased thickness results in the formation of topographic relief and a supporting crustal root. The development of topographic relief in the orogen results in erosion. Lastly, removal of material from the deformed zone by erosion reduces crustal thickness, changing again the equilibrium position of the deformed crustal block. This four-step process – deformation, isostatic compensation, erosion, isostatic rebound – is used to investigate the progressive development of topography and crustal root thickness.

Although transpression involves three-dimensional flow, evaluation of isostasy and erosion can be accomplished with a two-dimensional model. In transpression, the amount of vertical elongation is solely a function of the amount of horizontal shortening (Sanderson and Marchini, 1984). Exclusion of the transcurrent component of deformation allows the model to only consider the two-dimensional contractional component of deformation. Moreover, modifications to include the effects of isostatic compensation and erosion are one-dimensional because only the vertical component of flow is altered by these factors.

A strict interpretation of our sequence of operations results in the material points rising first due to contraction, then sinking due to isostatic forces, and then lastly rising again due to isostatic rebound after erosion (Fig. 2). If we assume that isostatic equilibrium is reached instantaneously (see Section 5.4 for discussion), then in the natural world all of these processes operate simultaneously. The step-wise approach taken here only approaches the actual simultaneous nature of these processes if the steps are sufficiently small. In development of the model step sizes ranging from 1000 yrs/step to 100,000 yrs/step were investigated. The model results stabilized at approximately 20,000 yrs/step, indicating that artifacts due to the step-wise approach were no longer significant in this time frame. Further reduction to a 1000 yrs/step increases computation time, but did not change model results. All results presented here use a step size of 10,000 yrs/step or less.

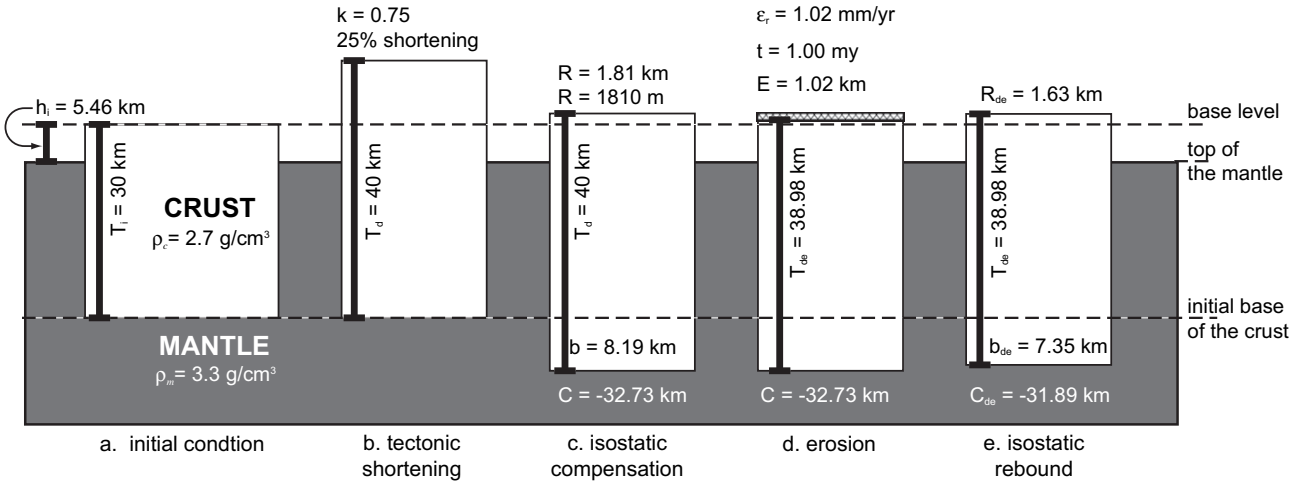

Fig. 2. Schematic diagram showing the four-step process used to incorporate isostatic compensation and erosion in transpression. See text for an explanation of variables.

2.1. Contraction in transpression

First, the plate boundary system is deformed by applying transpression to a zone of finite width. The deformation matrix that describes the movement of material points in monoclinic transpression is given by Tikoff and Fossen (1993) as

$$D = \begin{pmatrix} 1 & \Gamma & 0 \\ 0 & k & 0 \\ 0 & 0 & \frac{1}{k} \end{pmatrix}. \quad (1)$$

The coordinate system for this matrix is defined with a horizontal x-axis parallel to the shear zone or plate boundary, a horizontal y-axis perpendicular to the shear zone boundary, and a vertical z-axis (Fig. 1). The transcurrent component of deformation is described by Γ. Assuming a constant volume system, k is a value less than one that describes the shortening perpendicular to the shear zone boundary and $1/k$ describes the elongation in the vertical dimension.

The contractional component of deformation is of primary interest to this study, therefore Equation (1) can be simplified to examine two-dimensional material flow in the YZ plane (Fig. 1):

$$D_{yz} = \begin{pmatrix} k & 0 \\ 0 & \frac{1}{k} \end{pmatrix}. \quad (2)$$

This deformation matrix can be subdivided in a series of equal increments describing a kinematic steady-state deformation following Tikoff and Fossen (1993).

2.2. Isostatic compensation

Inclusion of isostasy into transpression affects flow only in the vertical dimension – i.e. the z-position of material points. The Airy isostasy relationship

$$h = T\left(\frac{\rho_m - \rho_c}{\rho_m}\right), \quad (3)$$

links the height of a block of crust (h) above a datum to the thickness of that block (T), the density of the crust (ρ_c), and the density of the mantle (ρ_m; e.g. Stüwe, 2002, Eq. 4.20, p. 153). Models of isostasy quantify the equilibrium level to which a solid block of material will rise above the surface of a liquid in which it is floating. With an iceberg, the less dense ice floats a height h above the more dense water – i.e. water level is the datum. In a tectonic system, a block of less dense crust floats a height h above the more dense mantle. This datum, however, is awkward to use because unlike water in the iceberg example, the mantle never reaches the surface. Our model assumes the theoretical top of the mantle is fixed in space and the crust moves with respect to this datum in response to isostasy. Therefore, we define the initial crustal height (h_i) as the isostatically compensated, equilibrium height of the initial crustal thickness (T_i) prior to deformation (Fig. 2a). The system starts with no topographic relief – i.e. the future transpressional zone is flat with an elevation equal to that of base level.

At the plate boundary scale, the vertical elongation component of transpression changes the initial thickness of the crust (T_i), which disturbs the isostatic equilibrium of the deformed zone (Fig. 2b). The thickness of the deformed crust (T_d) can then used to determine the height of the deformed zone (h_d) above the top of the mantle using equation (3) (Fig. 2c). With respect to base level, the topographic relief (R), the thickness of the crustal root (b), and the depth of the crustal root (C) are given by

$$R = h_d - h_i, \quad (4)$$

$$b = T_d - T_i - R, \text{ and} \quad (5)$$

$$C = h_i - T_i - b. \quad (6)$$

2.3. Erosion

The uplift of material and creation of a mountain range will result in erosion. The amount of erosion depends of the erosion rate and the duration of erosion. In this model, topographic relief (R) in meters is related to the rate of erosion (ε_r) in mm/yr by the equation

$$\varepsilon_r = 1.4 \times 10^{-6}(R)^{1.8}. \quad (7)$$

(Fig. 5 of Montgomery and Brandon, 2002). To include some estimate of the range of possible relief–erosion rate relationships into our model calculations, we included one standard deviation from Montgomery and Brandon (2002) for both the coefficient and the exponent in Eq. (7) giving the following equations:

$$\varepsilon_r = 4.9 \times 10^{-7}R^{1.6}, \text{ and} \quad (8)$$

$$\varepsilon_r = 4.1 \times 10^{-6}R^{2}. \quad (9)$$

The total amount of erosion (E) for a given increment of deformation is described by

$$E = \varepsilon_r t, \quad (10)$$

where t is the length of time of the increment of deformation (Fig. 2d).

2.4. Isostatic rebound due to erosion

The reduction in crustal thickness due to erosion disturbs the isostatic equilibrium of the deformed crust. The new thickness of the deformed crust after deformation and erosion (T_{de}) is given by

$$T_{de} = T_d - E. \quad (11)$$

Inserting this revised crustal thickness into equation (3) allows for the calculation of the height of the crustal block above the top of the mantle (h_{de}). The isostatically compensated topographic relief for the system after both deformation and erosion (R_{de}) is calculated using equation (4). Similarly, a revised root thickness (b_{de}) and depth (C_{de}) are determined using equations (5) and (6) (Fig. 2e).

2.5. Vertical flow

As originally conceived by Sanderson and Marchini (1984), the origin of the Cartesian coordinate system in a transpressional deformation is at the base of the shear zone (Fig. 1). The vertical flow of material in such a system applied at the lithospheric scale results in all of the material flowing upward and forming topography (Fig. 3b). Isostatic compensation, however, results in a shift of all material in the deforming zone downwards. The amount of downward flow is determined by the thickness of the crustal root and is described by

$$z' = z - b_{de}, \quad (12)$$

where z is z-position of a material point after deformation and z' is the z-position of a material point after isostatic compensation (Fig. 3c).

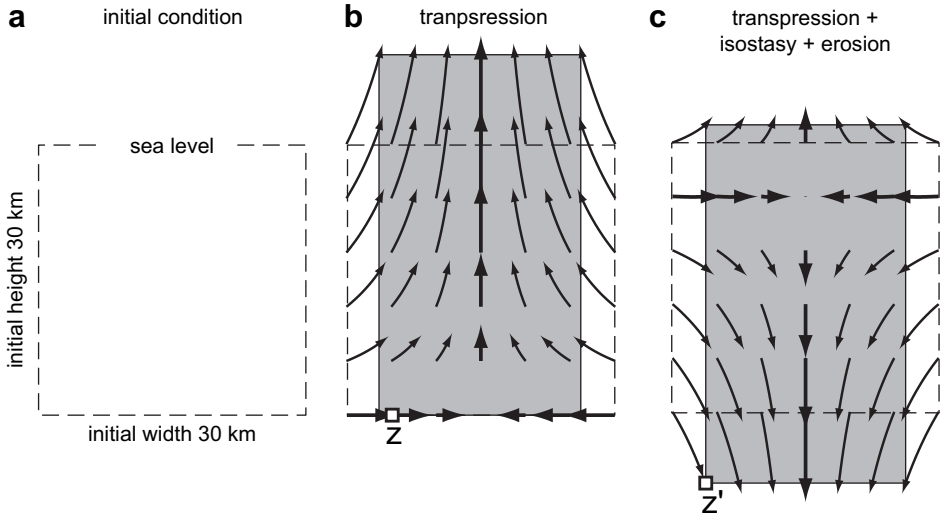

Fig. 3. Flow in the vertical plane of transpression. The bold flow lines track material points along the convergent and divergent flow apophyses. The box marked z denotes the position of an arbitrary material point after deformation. z' denotes the position of the same point in a system that includes isostasy and erosion.

3. Model results

The addition of isostasy and erosion into the two-dimensional, contractional system described above yields results that are more consistent with mountain building in natural systems than traditional transpressional models (Fig. 3). Instead of the material flowing upward, isostatic compensation results in most of the material in the transpressional zone flowing downward to develop a crustal root. A smaller amount of material flows upward to produce topography and is partially eroded away. We investigate the details of the relationship between tectonic shortening, development of topographic relief, and crustal root formation in transpression in the context of four variables: strain rate, erosion rate, initial crustal thickness, and density contrast. Model results are presented using two graphs: low strain (<25% shortening) and high strain systems (<75% shortening; Figs. 4–8).

3.1. Strain rate

The strain rate used in the model can affect topographic relief and crustal root development by controlling the rate of vertical flow. Higher strain rates tend to develop higher topographic relief and thicker crustal roots (Fig. 5). Strain rates are varied within the model by changing either the rate of convergence or the width of the deforming zone. For a shear zone with a given width, faster convergence rates result in a higher strain rate. Faster convergence rates result in higher topography and thicker crustal roots since erosion is less able to keep pace with the emerging topography (Fig. 4). Narrower zones also increase the strain rate and have the same effect (Fig. 5). To change the relationship between topographic relief and percent shortening by more than ±1% shortening, the rate of convergence or width of the zone must vary by an order of magnitude. The same is true of the crustal root–shortening relationship.

3.2. Erosion rate

Erosion rate is strongly dependent on the relief of an orogen (e.g. Montgomery and Brandon, 2002), therefore erosion rates must increase as topography emerges within the deforming zone. The range of empirically derived functions given in Eqs. (7)–(9) (Montgomery and Brandon, 2002) all produce similar results (Fig. 6).

3.3. Initial crustal thickness

Fig. 7 shows the results of varying the initial crustal thickness from 20 to 40 km. Topography and crustal root thickness are highly dependant on the initial thickness of the crust in a transpressional zone. The effect of initial thickness is apparent even for very low

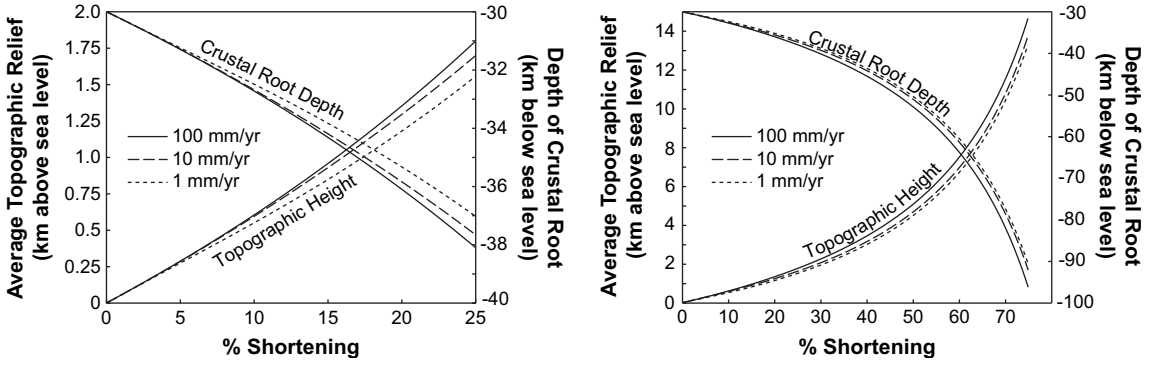

Fig. 4. Effect of rate of convergence. The final width of the zone is held constant at 100 km, the mean relief vs. erosion rate relation (Eq. (7)) is used, the initial thickness of the crust is set at 30 km, and the density contrast is set at 0.6 g/cm^3.

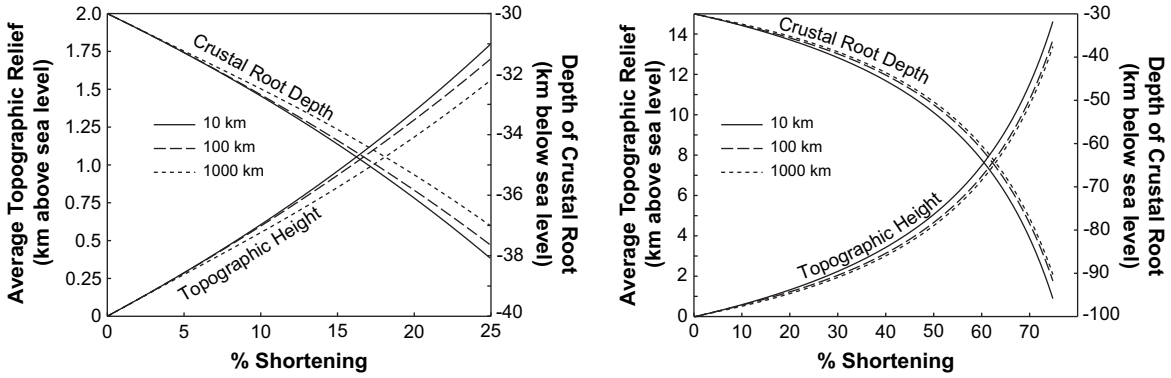

Fig. 5. Effect of the final width of the deforming zone. The rate of convergence is held constant at 10 mm/yr, the mean relief vs. erosion rate relation (Eq. (7)) is used, the initial thickness of the crust is set at 30 km, and the density contrast is set at 0.6 g/cm^3.

strains (i.e. <5% shortening). The greater the initial thickness of the crust, the more quickly the topography grows due to the greater volume of material available for creation of a supporting root.

3.4. Density contrast

The crust–mantle density contrast also has a strong effect on topographic and crustal root development (Fig. 8). When the density contrast is high, ~0.8 g/cm^3, isostasy forces the crust to float high in the system, creating greater topographic relief and a thinner crustal root. In contrast, low density contrasts, ~0.4 g/cm^3, create thicker crustal roots with minimal topography. In general, the density contrast affects the topographic relief more than the crustal root and the effects are notable even in low strain systems (<5% shortening).

4. Quantitative constraints on neotectonic contraction

A set of generalized nomograms showing the relation between tectonic shortening, average topographic relief, crustal root thickness, zone width, initial crustal thickness, and density contrast are presented in Fig. 9. For these plots, the rate of convergence is held constant at 10 mm/yr and the mean relief vs. erosion rate equation (Eq. (7)) of Montgomery and Brandon (2002) is used. We first apply the model results to a well-constrained transpressional setting that has independent strain estimates: the Alpine fault zone in New Zealand. Secondly, the model is applied to a less well known transpressional setting, the Central Range fault system in Trinidad, to illustrate the potential of our method to provide first-order estimates of the magnitude of neotectonic shortening.

4.1. Application to New Zealand

The Alpine fault system in New Zealand is an ideal plate boundary to apply our model results because the kinematics are well constrained based on fracture zone analysis (Cande and Stock, 2004) and GPS (Beavan et al., 2002, 2007). The plate reconstruction of Cande and Stock (2004) suggests convergence on the South Island of New Zealand began ~11 Ma at rates varying from 4 to 6 mm/yr and resulted in a 40 ± 15 km of shortening. These shortening values are less than the 90 ± 20 km estimated by Walcott (1998) also based on fracture zone data (Cande et al., 1995), a discrepancy that arises from the inclusion of the previously unrecognized Macquarie microplate in the analysis by Cande and Stock (2004). GPS data suggest that the modern rate of convergence ~9 mm/yr distributed over a 100 km wide zone (Fig. 10; Beavan et al., 2002). The NUVEL-1A model suggests 10 mm/yr of convergence on the Alpine fault (DeMets et al., 1990, 1994).

The Southern Alps mountain range is the topographic expression of the Pacific–Australia plate collision on the South Island of New Zealand. The elevation of the crest of the Southern Alps (i.e. the drainage divide) is a measure of the average topographic relief of the orogen. Based on the Shuttle Radar Topography Mission digital elevation data (available from U.S. Geological Survey, EROS Data Center, Sioux Falls, SD), the average elevation of the drainage divide on the central South Island is ~1.7 km above sea level. These mountains are underlain by a wide, asymmetric, triangular shaped

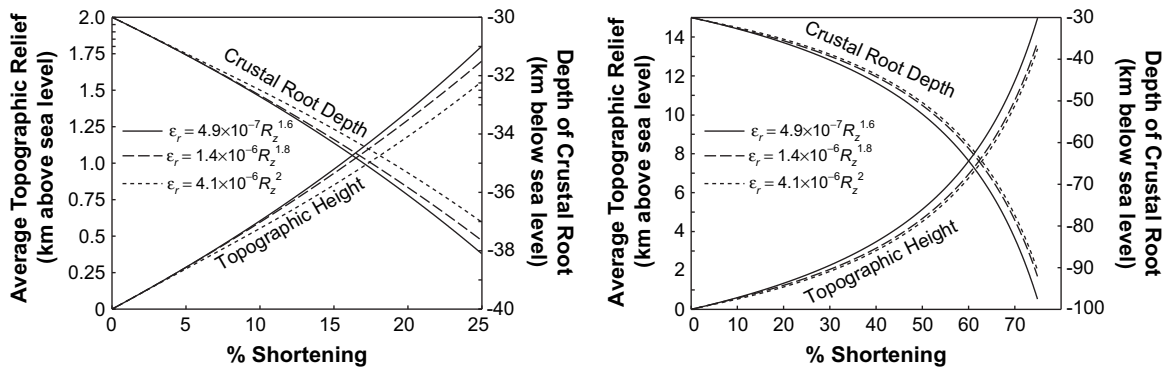

Fig. 6. Effect of the relief vs. erosion rate relationship (Eqs. (7), (8), or (9)). The rate of convergence is held constant at 10 mm/yr, final width of the zone is set at 100 km, the initial thickness of the crust is set at 30 km, and the density contrast is set at 0.6 g/cm^3.

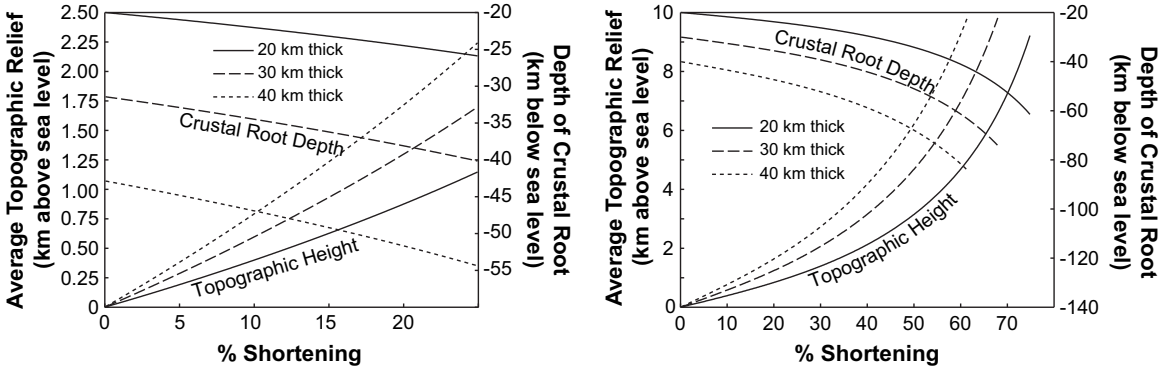

Fig. 7. Effect of initial crustal thickness. The rate of convergence is held constant at 10 mm/yr, final width of the zone is set at 100 km, the mean relief vs. erosion rate relation (Eq. (7)) is used, and the density contrast is set at 0.6 g/cm^3.

crustal root (Reilly and Whiteford, 1979; Davey et al., 2007; Bourguignon et al., 2007) that is thought to be composed primarily of metamorphosed sedimentary rocks (e.g. Walcott, 1998). At the coast, the continental crust is ~25–30 km thick and reaches a thickness of 40–50 km underneath the high topography of the Southern Alps (Davey et al., 2007; Bourguignon et al., 2007).

The values noted above place constraints on the initial thickness of the crust (25–30 km), the rate of convergence (4–10 mm/yr) and the present-day width of the deforming zone (100 km) in New Zealand. Metamorphic rocks have a wide variety of densities (2.5–2.9 g/cm^3), which gives a range of possible density contrasts (0.4–0.8 g/cm^3) when compared to peridotite mantle (3.3 g/cm^3). Based on an average divide height of 1.7 km and a crustal root depth of 45 km, model results predict 26–42% shortening and 51–66% shortening, respectively (Fig. 9). These values suggest 55 ± 20 km (topography) or 150 ± 50 km (crustal root) of shortening in a zone that is presently 100 km wide.

4.2. Application to Trinidad

The southeastern Caribbean island of Trinidad lies on the boundary between the South American plate and the Caribbean plate (Fig. 10). Relative to a fixed South America, the Caribbean plate is moving 20 mm/yr approximately due east (Perez et al., 2001; Weber et al., 2001). West of Trinidad, in Venezuela, most of this motion is accommodated by the El Pilar fault system (Perez et al., 2001). In Trinidad, plate motion has stepped to the south off of the El Pilar fault system into the Central Range fault system (Saleh et al., 2004). Based on GPS resurvey of a 1903 triangulation network in 1994 and campaign GPS data since then, 12 ± 3 mm/yr of the total 20 mm/yr of relative plate motion is thought to be accommodated by the Central Range fault system (Weber et al., 2002). This rate is slower than the 17–19 mm/yr Holocene average determined by Soto et al. (2007).

The Central Range fault system is approximately 40 km wide (Saleh et al., 2004) and strikes approximately N70E, which is 20° oblique to the approximately N90E Caribbean plate motion vector (Weber et al., 2002). Plate motion of 12 mm/yr oriented 20° oblique to the Central Range fault zone yields 4 mm/yr zone normal convergence (Saleh et al., 2004). This convergence has lead to the development of the Central Range Mountains, which have an average divide height of 160 m based on digital elevation data from the Seamless Shuttle Radar data set (available from U.S. Geological Survey, EROS Data Center, Sioux Falls, SD).

The amount of strain recorded by the modern tectonic system is unknown primarily because the Caribbean plate lacks a major spreading center, therefore it is not possible to use fracture zone analysis to analyze recent plate motion (e.g. DeMets et al., 1990). Additionally, the Central Range was the locus of Miocene age contraction (e.g. Algar and Pindell, 1993; Pindell and Lorcan, 2002), therefore the role of folding and faulting in central Trinidad due to Miocene contraction vs. modern transpression is difficult to determine.

The values noted above place constraints on the rate of convergence (4 mm/yr) and the present-day width of the deforming zone (40 km) in Trinidad. Precise estimates of the initial crustal thickness are not available, therefore we assume a thickness between 20 and 30 km. Similarly, the density of the crust in Trinidad is unknown. The surficial strata consist of Tertiary passive margin sediments and deposits of the Orinoco delta system (e.g. Kugler, 1959). These sediments are likely underlain by crystalline metamorphic or igneous rocks. Therefore we investigate a range of

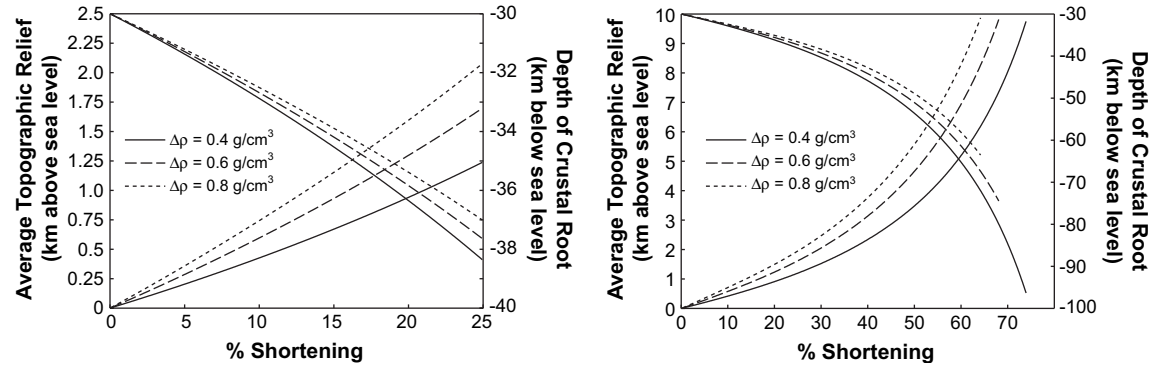

Fig. 8. Effect of crust–mantle density contrast. The rate of convergence is held constant at 10 mm/yr, final width of the zone is set at 100 km, the mean relief vs. erosion rate relation (Eq. (7)) is used, and the initial thickness of the crust is set at 30 km.

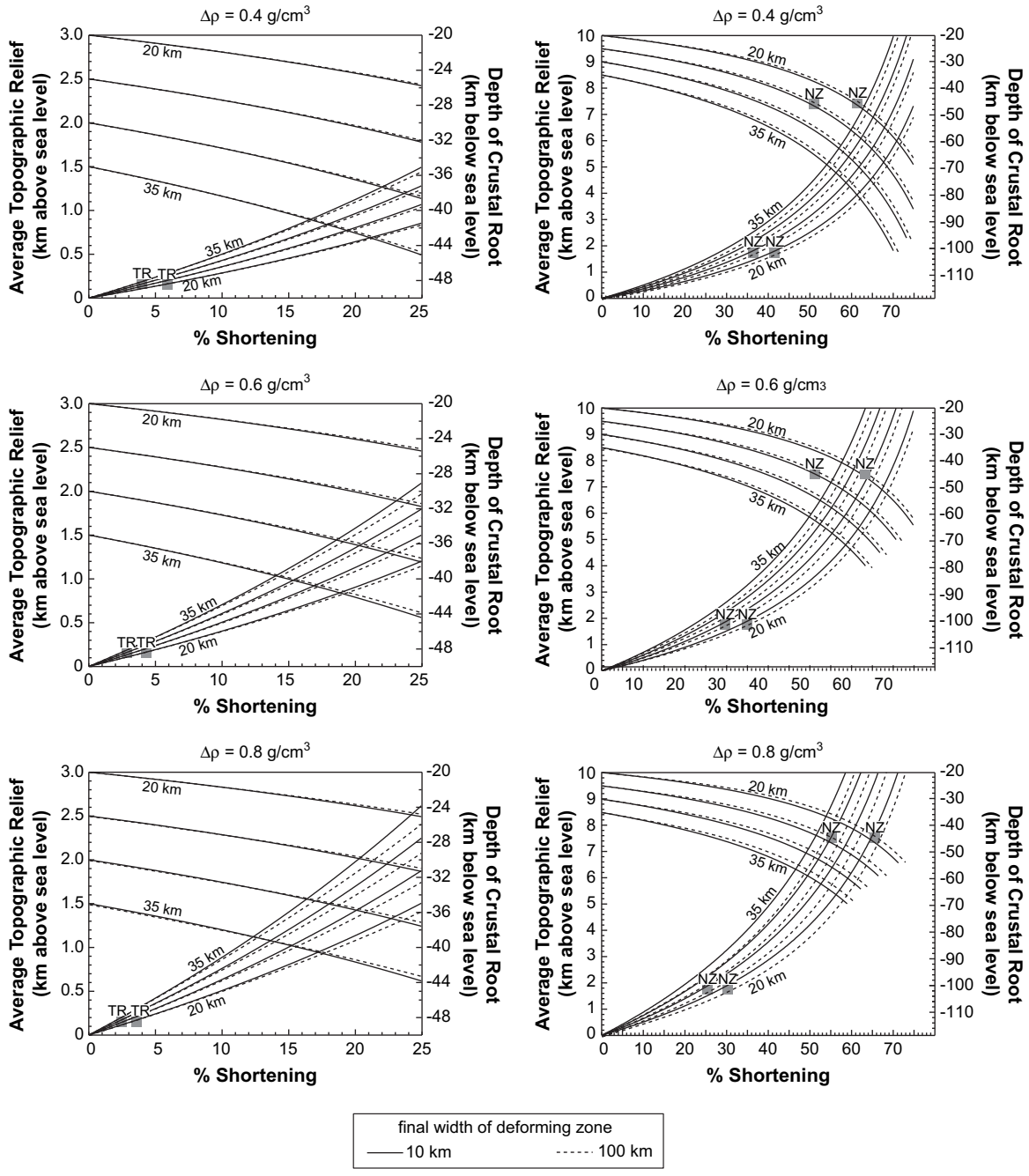

Fig. 9. Graphs estimating the percent shortening in a transpressional belt from the average topographic relief and/or crustal root depth. The graphs depict the model results for three different density contrasts for both low strain and high strain. Within each graph the results for initial continental thicknesses of 20, 25, 30, and 35 km are shown. In all cases the rate of convergence is held constant at 10 mm/yr and the mean relief vs. erosion rate equation is used (Eq. (7)). A range of possible strain analysis results are presented for the Alpine fault system in New Zealand (NZ) and the Central Range fault system in Trinidad (TR).

density contrasts from 0.4 to 0.8 g/cm^3. Using an average divide height of 160 m, the Central Range fault system has experienced 3–6% shortening (Fig. 9), which is equivalent to 2 ± 1 km of shortening across a presently 40 km wide zone.

5. Discussion

Incorporation of isostasy and erosion into transpression offers an opportunity to use widely available data sets (digital topography and gravity data) as the basis for strain analysis (Fig. 9). Application to the central South Island of New Zealand produces promising topography-based model results (55 ± 20 km of shortening) that overlap with those derived from plate reconstructions (45 ± 15 km; Cande and Stock, 2004). Estimation based on the crustal root depth, however, produces much less compelling results (150 ± 50 km). In discussion below we first examine this discrepancy. Secondly, we discuss the simplifying assumptions need to develop this strain analysis technique. We examine the potential effects of flow geometry, homogeneous strain, isostatic equilibrium, boundary-parallel stretch, and strain history on the interpretation of our model results as a measure of natural strain.

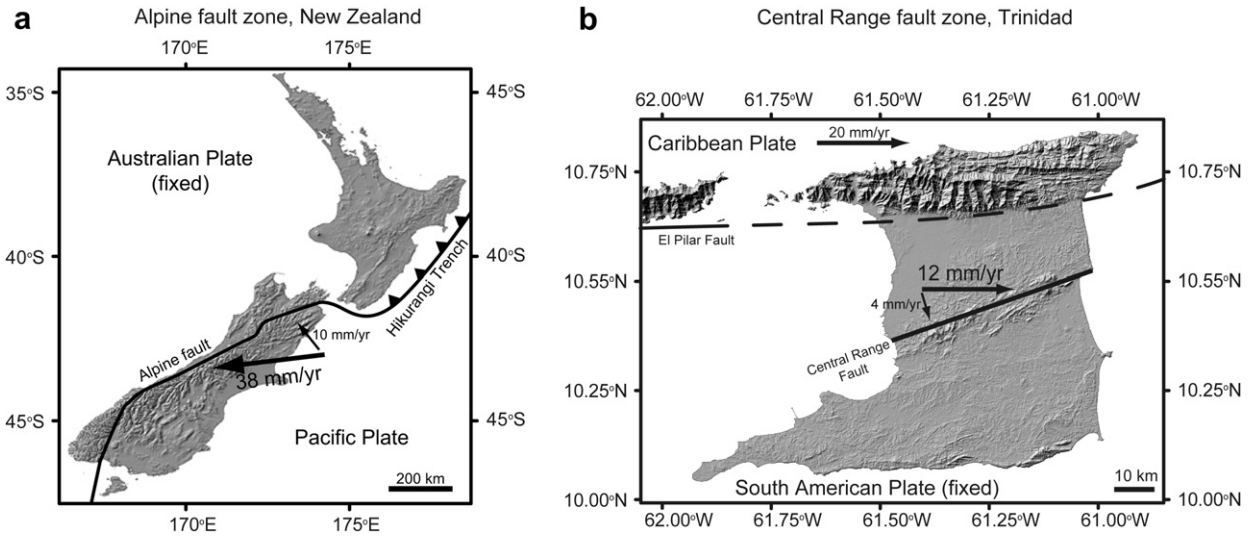

Fig. 10. a) Map of New Zealand. The Pacific plate is moving 38 mm/yr relative to a fixed Australian plate at an angle of approximately 16° to the Alpine fault, which results in 10 mm/yr of convergence (plate motions from DeMets et al., 1990, 1994; map modified from Walcott, 1998). b) Map of Trinidad. The Caribbean plate is moving 20 mm/yr due east relative to a fixed South American plate, which results in a 20° angle of oblique convergence in the Central Range. Approximately 12 mm/yr of that motion is accommodated by the Central Range fault zone, resulting in 4 mm/yr of convergence (plate motions from Weber et al., 2001; Saleh et al., 2004; map modified from Weber, 2007). Shaded relief images in both maps were generated using the Seamless Shuttle Radar data (available from U.S. Geological Survey, EROS Data Center, Sioux Falls, SD).

5.1. Topography vs. crustal root

Model results from New Zealand favor the use of topographic data over crustal root data as the basis for the strain analysis for two reasons. First, crustal root-based estimates of strain are highly sensitive to the assumed initial thickness of the crust. Regardless of the initial crustal thickness, the height of the topography always starts in the same place: zero meters above sea level (Fig. 7). The starting point for crustal root development, however, directly depends on the assumed initial crustal thickness (Fig. 7). Therefore, precise knowledge the initial thickness of the crust is needed to generate crustal root-based results that have uncertainties equivalent to topography-based results (Fig. 9). Secondly, there is a much greater uncertainty in the crustal root depth than in the topographic data set. Digital elevation data sets such as the Shuttle Radar data set have measurement uncertainties that are on the order of meters, while the uncertainties associated with the crustal root depth are on the order of kilometers (Davey et al., 2007; Bourguignon et al., 2007). The seismic and gravity data sets from New Zealand are high quality and probably represent a best case scenario for the use of crustal root thickness to estimate tectonic shortening. Therefore, shortening estimates based on crustal root depth are of limited utility. However, as noted below, knowledge of the size of the crustal root is still useful with respect to the analysis presented here because it is necessary to determine if the orogen is in isostatic equilibrium.

5.2. Flow geometry

The addition of isostasy and erosion into transpression changes the distribution of vertical flow, but does not alter the geometry of flow – i.e. the angle between the flow apophyses remains the same (Fig. 3). Similarly, the geometry of the flow lines relative to the flow apophyses does not change (Fig. 3), therefore the shape and orientation of the strain ellipsoid are not changed by the incorporation of isostasy and erosion into transpression. Assuming that fabrics are a reflection of the strain ellipsoid, then the foliation and lineation orientations in transpression with isostasy and erosion should be identical to those predicted in the original transpressional model (e.g. Sanderson and Marchini, 1984; Fossen and Tikoff, 1993).

5.3. Homogeneous strain

Model results are based on the Sanderson and Marchini (1984) model of transpression that assumes homogeneous strain and produces a "flat topped" mountain range (Fig. 3). In natural transpressional systems, shortening is likely to be partitioned across the orogen and along strike. Partitioning of shortening should result in variations in topographic relief throughout the orogen. In New Zealand, topographic relief clearly varies along strike, as does the amount of tectonic shortening (e.g. Walcott, 1998; Cande and Stock, 2004). Similarly, topography varies across the orogen, as does the intensity of deformation (e.g. Koons, 1994; Beavan et al., 2002). Variation in crustal root thickness follows a similar pattern (e.g. Davey et al., 2007; Bourguignon et al., 2007). A homogeneous strain assumption averages deformation throughout the orogen, therefore topographic relief must be quantified at the orogen scale rather than at a local scale. In our analysis, we use the average elevation of the drainage divide as a measure of the average topographic relief on the orogen scale. The strain analysis results for New Zealand and Trinidad are based on orogen-wide measures of topographic relief and/or crustal root thickness, therefore the results are best interpreted as general, first-order estimates for the entire orogen rather than any specific local within the orogen.

5.4. Isostatic equilibrium

Our model assumes the zone of deformation achieves isostatic equilibrium instantaneously and remains in isostatic equilibrium throughout the deformation. Natural systems may be in some state of disequilibrium with respect to isostasy. Consider the following two scenarios. First, suppose that the crustal root was larger than expected for a given amount of topography. Application of our model results to an "excessively large" crustal root would yield an overestimation of the tectonic shortening. This same scenario could be described as having a mountain range that was too low topographically for a given root size. Application of the model to the

"abnormally small" mountain range leads to an underestimation of the tectonic shortening. The second scenario is the exact opposite: the crustal root is either too small or the mountain range too large. This results in an underestimation of strain based on crustal root thickness and an overestimation based to topography. Both scenarios illustrate the necessity of having some understanding of the present-day state of isostatic equilibrium in an orogen to apply the model results in a meaningful way. For example, the 40–50 km thick crustal root of the Southern Alps is larger than expected for the topography (Davey et al., 2007; Bourguignon et al., 2007). This indicates that the 55 ± 20 km of shortening predicted from the topography is a minimum and the 150 ± 50 km based on the crustal root thickness is a maximum. A lack of seismic or gravity data from Trinidad prevents us from assessing the isostatic state of the Central Range. Therefore it is unknown if the very small amount of shortening calculated based on topography (2 ± 1 km) is a minimum or a maximum.

5.5. Boundary-parallel stretch

Two-dimensional strain analysis requires all deformation to occur in the plane analyzed. In transpression the contractional component is contained in the *YZ* plane and stretching parallel to the shear zone boundary is absent (the *x*-axis in Fig. 1; Sanderson and Marchini, 1984). Material flow parallel to the shear zone boundary does not result in a topographic signal and therefore will not manifest itself as a change in topography or a crustal root thickness.

For the Alpine fault system, this simple situation may not apply because evidence exists for interpreting the presence of boundary-parallel stretching (Walcott, 1998). If so, the model results should underestimate the amount of shortening in this transpressional system. The results overlap or exceed those suggested by shortening values derived from plate reconstruction (Cande and Stock, 2004), suggesting that the magnitude of any boundary-parallel stretching component in the Alpine fault system is within the uncertainties of our analysis.

5.6. Erosion rate

The relief vs. erosion rate functions used in this numerical model are empirically derived from erosion rate estimates from a wide variety of tectonic settings. As noted by Montgomery and Brandon (2002), these functions tend to underestimate the erosion rate in active, high relief orogens (i.e. >1000 m of relief). The Southern Alps is a high relief system, therefore the model probably underestimates the rate of erosion, which leads to an underestimate of the amount of flow in the vertical dimension and an underestimation of the amount of horizontal shortening. Thus, shortening values based on topography in high relief orogens may be minimum estimates. Trinidad is a much lower relief orogen, therefore the relief vs. erosion rate relation of Montgomery and Brandon (2002) is probably a reasonable approximation.

5.7. Strain history

Finite strain analysis provides information about the total deformation, but does not provide explicit information about different increments of deformation throughout the history of a shear zone (e.g. Elliott, 1972; Passchier, 1988; Jiang and White, 1995). Unlike many strain markers, mountains and their supporting crustal root are transient features. After the tectonic forces driving mountain building cease, the mountains erode and the crustal root rebounds and eventually disappears. In a sense these features "anneal" with time. Therefore, an advantage of strain analysis based on topography/crustal root depth is that it provides finite strain information about only the most recent, ongoing episode of deformation. Since fault zones and plate boundaries are often repeatedly reactivated throughout their history (e.g. Vauchez et al., 1997; Rutter et al., 2001), the approach presented here is potentially valuable as a tool for distinguishing between neotectonic and ancient tectonic strain. For example, the folding and faulting in the Central Range of Trinidad could be the result of neotectonic transpression (Weber et al., 2002; Saleh et al., 2004) and/or Miocene contraction (e.g. Algar and Pindell, 1993). It is difficult to determine which structures are associated with either or even both events. However, the transient nature of topography and the present-day low relief (<300 m) in the Central Range suggest that these mountains are most likely the result of the modern transpressional plate motion (e.g. Weber et al., 2001) rather than the older Miocene age deformation (e.g. Algar and Pindell, 1993). Therefore we would interpret the 2 ± 1 km of shortening suggested by the model as resulting from neotectonic deformation.

6. Conclusions

Incorporation of isostatic compensation and erosion into a kinematic model of transpression creates a more realistic picture of the effects of plate boundary-scale transpression. Without including isostasy, deformation results in unrealistically high topography without a supporting crustal root. Isostatic effects and erosion reduce these heights to a more realistic level with a thick supporting crustal root. When applied to orogens at the plate boundary scale, our model suggests that most material in a transpressional zone will flow downward into a crustal root. Incorporation of isostasy and erosion into transpression does not, however, change the overall strain geometry or fabric orientations that develop in transpressional flow.

Analysis of the Alpine fault system using this model suggests it is possible to use topographic relief as a strain marker in neotectonic obliquely convergent settings. The topography suggests 55 ± 20 km of shortening, a value that overlaps previous estimates arrived at through fracture zone analysis (45 ± 15 km; Cande and Stock, 2004). Application of the model results to the much less well-constrained Central Range fault system in Trinidad suggests the low relief hills of the Central Range Mountains in Trinidad record 2 ± 1 km of modern shortening.

Isostatically compensated transpressional provides a strain analysis tool for modern, active transpressional boundaries (Fig. 9). The uncertainty associated with this strain analysis method can be reduced with precise estimates of the crust–mantle density contrast and the initial, undeformed crustal thickness. Order of magnitude estimates of the convergence rate and width of the deforming zone are also required. Information about isostatic equilibrium, boundary-parallel stretch, and erosion rates will also increase the confidence with which of the strain estimate can be interpreted as a maximum or minimum amount of shortening. Topography-based strain analysis may be most useful in neotectonic settings that (1) lack other strain markers and/or (2) reactivate older orogenic belts making it unclear how much of the strain recorded in the rock record is due to neotectonic vs. ancient contraction.

Acknowledgments

This manuscript has been greatly improved by discussions with Eric Horsman, Sarah Titus, and John Weber. We thank David Sanderson, an anonymous reviewer, and William Dunne for helpful and constructive criticism. Acknowledgment is made to the Donors of the American Chemical Society Petroleum Research Fund for partial support of this research.

References

Algar, S.T., Pindell, J., 1993. Structure and deformation history of the northern range of Trinidad and adjacent areas. Tectonics 16, 814–829.

Argus, D.F., Gordon, R.G., 2001. Present tectonic motion across the coast ranges and San Andreas fault system in central California. Bulletin of the Geological Society of America 113, 1580–1592.

Beaumont, C., Fullsack, P., Hamilton, J., 1992. Erosional control of active compressional orogens. In: McClay, K.R. (Ed.), Thrust Tectonics. Chapman & Hall, London, pp. 1–18.

Beavan, J., Tregoning, P., Bevis, M., Kato, T., Meertens, C., 2002. Motion and rigidity of the pacific plate and implications for plate boundary deformation. Journal of Geophysical Research B: Solid Earth 107.

Beavan, J., Ellis, S., Wallace, L., Denys, P., 2007. Kinematic constraints from GPS on oblique convergence of the Pacific and Australian Plates, central South Island, New Zealand. In: Okaya, D.A., Stern, T., Davey, F.J. (Eds.), A Continental Plate Boundary: Tectonics at South Island, New Zealand. Geophysical Monograph 175, pp. 75–94.

Bourguignon, S., Savage, M.K., Stern, T., 2007. Crustal thickness and Pn anisotropy beneath the Southern Alps oblique collision, New Zealand. In: Okaya, D.A., Stern, T., Davey, F.J. (Eds.), A Continental Plate Boundary: Tectonics at South Island, New Zealand. Geophysical Monograph 175, pp. 115–122.

Cande, S.C., Raymond, C.A., Stock, J., Haxby, W.F., 1995. Geophysics of the Pitman fracture zone and Pacific–Antarctic plate motions during the Cenozoic. Science 270, 947–953.

Cande, S.C., Stock, J.M., 2004. Pacific–Antarctic–Australia motion and the formation of the Macquarie plate. Geophysical Journal International 157, 399–414.

Davey, F.J., Eberhart-Phillips, D., Kohler, M.D., Bannister, S., Caldwell, G., Henrys, S., Scherwath, M., Stern, T., Van Avendonk, H.J.A., 2007. Geophysical structure of the Southern Alps Orogen, South Island, New Zealand. In: Okaya, D.A., Stern, T., Davey, F.J. (Eds.), A Continental Plate Boundary: Tectonics at South Island, New Zealand. Geophysical Monograph 175, pp. 47–73.

DeMets, C., Gordon, R.G., Argus, D.F., Stein, S., 1990. Current plate motions. Geophysical Journal International 101, 425–478.

DeMets, C., Gordon, R.G., Argus, D.F., Stein, S., 1994. Effect of recent revisions to the geomagnetic time scale on estimates of current plate motions. Geophysical Research Letters 21, 2191–2194.

Dewey, J.F., Holdsworth, R.E., Strachan, R.A., 1998. Transpression and transtension zones. In: Holdsworth, R.E., Strachan, R.A., Dewey, J.F. (Eds.), Continental Transpressional and Transtensional Tectonics. Geological Society, London, Special Publications, vol. 135, pp. 1–14.

Elliott, D., 1972. Deformation paths in structural geology. Geological Society of America Bulletin 83, 2621–2638.

Fossen, H., Tikoff, B., 1993. The deformation matrix for simultaneous simple shearing, pure shearing, and volume change, and its application to transpression–transtension tectonics. Journal of Structural Geology 15, 413–422.

Jiang, D., White, J.C., 1995. Kinematics of rock flow and the interpretation of geological structures, with particular reference to shear zones. Journal of Structural Geology 17, 1249–1265.

Koons, P.O., 1994. Three-dimensional critical wedges: tectonics and topography in oblique collisional orogens. Journal of Geophysical Research 99, 12301–12315.

Kugler, H.G., 1959. Geological Map and Sections of Trinidad. The Petroleum Association of Trinidad, Port of Spain. 1:100,000 scale.

Little, T.A., Savage, M.K., Tikoff, B., 2002. Relationship between crustal finite strain and seismic anisotropy in the mantle, Pacific–Australia plate boundary zone, South Island, New Zealand. Geophysical Journal International 151, 106–116.

Montgomery, D.R., Brandon, M.T., 2002. Topographic controls on erosion rates in tectonically active mountain ranges. Earth and Planetary Science Letters 201, 481–489.

Passchier, C.W., 1988. Analysis of deformation paths in shear zones. Geologische Rundschau 77, 309–318.

Perez, O.J., Bilham, R., Bendick, R., Velandia, J.R., Hernández, N., Moncayo, C., Hoyer, M., Kozuch, M., 2001. Velocity field across the southern Caribbean plate boundary and estimates of Caribbean/South American plate motion using GPS geodesy 1994–2000. Geophysical Research Letters 28, 2987–2990.

Pindell, J., Lorcan, K., 2002. Tectonic model for Eastern Venezuela and Trinidad since 12 Ma. In: Annual Meeting Expanded Abstracts, vol. 3. American Association of Petroleum Geologists, p. 140.

Reilly, W.I., Whiteford, C.M., 1979. Gravity Map of New Zealand, 1:1,000,000, Bouguer and Isostatic Anomalies, South Island. Department of Scientific and Industrial Research, Wellington, New Zealand.

Robin, P.-Y.F., Cruden, A.R., 1994. Strain and vorticity patterns in ideally ductile transpressive zones. Journal of Structural Geology 16, 447–466.

Rutter, E.H., Holdsworth, R.E., Knipe, R.J., 2001. The nature and tectonic significance of fault-zone weakening; an introduction. In: Holdsworth, R.E., Strachan, R.A., Magloughlin, J.F., Knipe, R.J. (Eds.), The Nature and Tectonic Significance of Fault Zone Weakening. Geological Society, London, Special Publications, vol. 186, pp. 1–11.

Saleh, J., Edwards, K., Barbaste, J., Balkaransingh, S., Grant, D., Weber, J., Leong, T., 2004. On some improvements in the geodetic framework of Trinidad and Tobago. Survey Review 37, 604–625.

Sanderson, D.J., Marchini, W.R.D., 1984. Transpression. Journal of Structural Geology 6, 449–458.

Spotila, J.A., Niemi, N., Brady, R., House, M., Buscher, J., Oskin, M., 2007. Long-term continental deformation associated with transpressive plate motion; the San Andreas Fault. Geology 35, 967–970.

Soto, M.D., Mann, P., Escanola, A., Wood, A.J., 2007. Late Holocene strike-slip offset of a subsurface channel interpreted from three-dimensional seismic data, eastern offshore Trinidad. Geology 35, 859–862.

Stüwe, K., 2002. Geodynamics of the Lithosphere. Springer-Verlag, New York, 449 pp.

Stüwe, K., Barr, T., 1998. On uplift and exhumation during convergence. Tectonics 17, 80–88.

Teyssier, C., Tikoff, B., 1998. Strike-slip partitioned transpression of the San Andreas fault system: a lithospheric-scale approach. In: Holdsworth, R.E., Strachan, R.A., Dewey, J.F. (Eds.), Continental Transpressional and Transtensional Tectonics. Geological Society, London, Special Publications, vol. 135, pp. 143–158.

Thompson, A.B., Schulmann, K., Jezek, J., 1997. Thermal evolution and exhumation in obliquely convergent (transpressive) orogens. Tectonophysics 280, 171–184.

Tikoff, B., Fossen, H., 1993. Simultaneous pure and simple shear: the unifying deformation matrix. Tectonophysics 217, 267–283.

Vauchez, A., Barruol, G., Tommasi, A., 1997. Why do continents break-up parallel to ancient orogenic belts? Terra Nova 9, 62–66.

Walcott, R.I., 1998. Modes of oblique compression; late Cenozoic tectonics of the South Island of New Zealand. Reviews of Geophysics 36, 1–26.

Weber, J.C., 2007. Neotectonics in Trinidad and Tobago. In: Proceedings of the 4th Conference of the Geological Society of Trinidad and Tobago, 25 pp.

Weber, J.C., Dixon, T.H., DeMets, C., Ambeh, W.B., Jansma, P., Mattioli, G., Saleh, J., Sella, G., Bilham, R., Perez, O., 2001. GPS estimate of relative motion between the Caribbean and South American plates, and geological implications for Trinidad and Venezuela. Geology 29, 75–78.

Weber, J.C., Dixon, T., Prentice, C.S., 2002. Trinidad neotectonics from geodesy, geology, geomorphology and paleoseismology. In: Program and Abstracts of Papers – Caribbean Geological Conference, vol. 16, pp. 105–106.

Willett, S.D., 1999. Orogeny and orography: the effects of erosion on the structure of mountain belts. Journal of Geophysical Research 104, 28957–28981.

Willett, S.D., Brandon, M.T., 2002. On steady states in mountain belts. Geology 30, 175–178.